Science of the Total Environment 917 (2024) 170370

Contents lists available at ScienceDirect

Science of the Total Environment

journal homepage: www.elsevier.com/locate/scitotenv

Limitations of a biokinetic model to predict the seasonal variations of nitrous oxide emissions from a full-scale wastewater treatment plant

Siddharth Seshan [a,b,*], Johann Poinapen [a], Marcel H. Zandvoort [c], Jules B. van Lier [b], Zoran Kapelan [b]

[a] KWR Water Research Institute, Nieuwegein, the Netherlands
[b] Section Sanitary Engineering, Department of Water Management, Faculty of Civil Engineering and Geosciences, Delft University of Technology, Delft, the Netherlands
[c] Waternet, Amsterdam, the Netherlands

HIGHLIGHTS

- ASDM-N_2O model setup for full-scale WWTP and calibrated with long duration data
- Model predictions made for N_2O seasonal variations, inclusive of an emission peak
- Insights gained on prominent N_2O production pathways during the seasonal peak
- Free nitrous acid concentration can have a strong influence in N_2O production.
- Biokinetic model faces challenges in adequately simulating N_2O seasonal variations.

GRAPHICAL ABSTRACT

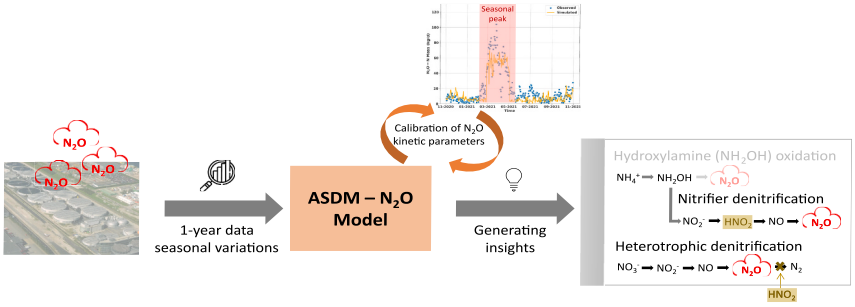

ARTICLE INFO

Editor: Huu Hao Ngo

Keywords:
Nitrous oxide
Production pathways
Seasonal variations
Biokinetic modelling
Free nitrous acid

ABSTRACT

A biokinetic model based on BioWin's Activated Sludge Digestion Model (ASDM) coupled with a nitrous oxide (N_2O) model was setup and calibrated for a full-scale wastewater treatment plant (WWTP) Amsterdam West, in the Netherlands. The model was calibrated using one year of continuous data to predict the seasonal variations of N_2O emissions in the gaseous phase. This, according to our best knowledge, is the most complete full-scale data set used to date for this purpose. The results obtained suggest that the currently available biokinetic model predicted the winter, summer, and autumn N_2O emissions well but failed to satisfactorily simulate the spring peak. During the calibration process, it was found that the nitrifier denitrification pathway could explain the observed emissions during all seasons while a combination of the nitrifier denitrification and incomplete heterotrophic denitrification pathways seemed to be dominant during the emissions peak observed during the spring season. Specifically, kinetic parameters related to free nitrous acid (FNA) displayed significant sensitivity leading to increased N_2O production. The obtained values of two kinetic parameters, i.e., the FNA half-saturation during ammonia oxidising bacteria (AOB) denitrification and the FNA inhibition concentration related to heterotrophic denitrification, suggested a strong influence of the FNA bulk concentration on the N_2O emissions and the observed seasonal variations. Based on the suboptimal performance and limitations of the biokinetic model, further research is needed to better understand the biochemical processes behind the seasonal peak and the influence of FNA.

* Corresponding author at: KWR Water Research Institute, Groningenhaven 7, 3430 BB Nieuwegein, the Netherlands.
E-mail address: siddharth.seshan@kwrwater.nl (S. Seshan).

https://doi.org/10.1016/j.scitotenv.2024.170370
Received 24 July 2023; Received in revised form 16 January 2024; Accepted 20 January 2024
Available online 26 January 2024

1. Introduction

As the effects of climate change and global warming are becoming more apparent, great efforts are being made to reduce the carbon footprint of industries and society. Nitrous oxide (N_2O) is considered a potent greenhouse gas (GHG), with its increasing atmospheric concentrations contributing to climate change (IPCC, 2014) and the depletion of the ozone layer in the stratosphere (Ravishankara et al., 2009). Furthermore, the global warming potential of N_2O is very high, 273 times greater than that of carbon dioxide (CO_2) on a 100-year time scale (Forster et al., 2021). Therefore, identifying and mitigating the anthropogenic sources of N_2O is crucial in curbing its harmful environmental effects.

Wastewater treatment plants (WWTPs) are increasingly considered to be one of the main sources of N_2O. The production of N_2O in WWTPs is associated with biological nitrogen removal (BNR) processes, more specifically the autotrophic nitrification and heterotrophic denitrification (Wunderlin et al., 2012). Three production pathways (as shown in Fig. 1) have been identified for its generation so far (Kampschreur et al., 2009; Massara et al., 2017a). It must be noted that within the nitrifier denitrification pathway, the nitrite (NO_2^-) formed due to the oxidation of ammonium (NH_4^+) by the ammonium oxidising bacteria (AOB), at certain pH conditions, can lead to the accumulation of free nitrous acid (HNO_2). At this point, HNO_2 can act as an electron acceptor leading to its reduction to nitric oxide (NO) and further to N_2O.

Given the diverse conditions and processes that induce N_2O emissions, detailed monitoring of N_2O and related parameters is necessary to better understand its production pathways. A small number of long-term monitoring campaigns have been reported so far, for both covered and open bioreactors (Chen et al., 2019; Daelman et al., 2015; Gruber et al., 2020; Gruber et al., 2021a; Kosonen et al., 2016). Higher emission factors (EFs), that is a percentage of influent nitrogen load emitted as N_2O, were reported from these campaigns than from the short-term ones (Daelman et al., 2015; Vasilaki et al., 2019). Furthermore, long duration measurement campaigns have reported distinctive seasonal and diurnal variations of the N_2O emissions (Daelman et al., 2013; Gruber et al., 2020; Kosonen et al., 2016). A significant seasonal peak has been recorded, typically during the spring months, with lower emissions being witnessed during autumn (Gruber et al., 2021a). The EFs during the seasonal peak were found to be as high as 11 %, compared to the annual average of 2.8 % (Daelman et al., 2015). Such a high contribution warrants better understanding of the causes behind the emissions peak (Gruber et al., 2021a).

Biokinetic models, such as ASM1 (Sin and Al, 2021) have been extended to also include the production pathways of N_2O, to predict its emission and to test control and mitigation strategies (Duan et al., 2021). The developed models include only one N_2O production pathway (Mampaey et al., 2013; Ni et al., 2011) to all three pathways (Massara et al., 2017b; Ni et al., 2015; Guo and Vanrolleghem, 2013). The modelling investigations were mostly carried out on datasets obtained from a controlled environment, such as lab-scale or pilot-scale setups, barring a handful of cases that used data from full-scale systems (Blomberg et al., 2018; Mampaey et al., 2019; Ni et al., 2015; Ni et al., 2013a; Spérandio et al., 2016). In the cases of full-scale based investigations, the duration of data used for the calibration purposes is typically short (often <1 month) to mid-term, missing seasonal variations hence resulting in limited predictive performance of the model when faced with unseen data containing the seasonal peak. To the best of the authors' knowledge, no biokinetic models reported in literature have been validated on data containing the seasonal peak from full-scale WWTPs nor attempts have been made to try and explain the underlying processes behind the peak(s) through biokinetic modelling.

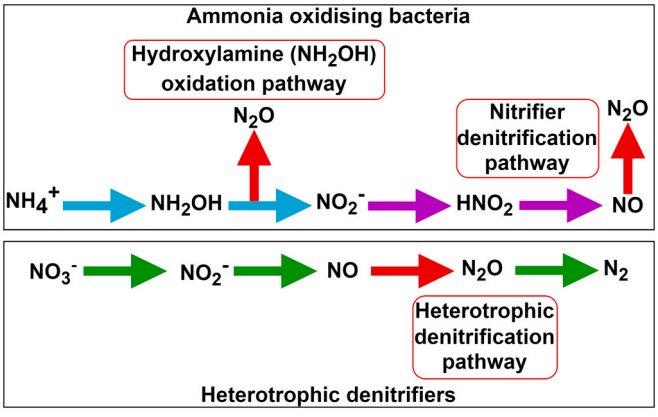

Fig. 1. The three production pathways of N_2O emissions associated with biological nitrogen removal in WWTPs.
Figure modified from Massara et al. (2017a).

Our presented research addressed the above knowledge gaps via the following research objectives. The first objective was to determine whether the accuracy of N_2O emissions predictions from an activated sludge/digestion model (ASDM) complemented with N_2O biokinetic equations can be improved, including a prediction of the seasonal peak (s). Any limitations of the biokinetic model preventing accurate predictions of the seasonal variations were identified. The second objective was to identify the kinetic parameters and their values that led to the prediction of the N_2O seasonal emission peak. The key elements of novelty in pursuing these objectives are as follows:

- Calibration of the biokinetic model using one year of observed N_2O emissions data from a full-scale WWTP. This, according to our best knowledge, is the most complete full-scale data set used to date for this purpose;
- Simulating the seasonal emissions peak to assess the model's capability in performing such predictions. This, according to our best knowledge has not been attempted so far;
- Improved understanding of the seasonal peak by identifying possible underlying biokinetic processes that trigger this peak.

2. Methodology

2.1. Overview

In Fig. 2, the methodology followed in this study is summarised. First, a comprehensive sampling campaign was conducted to obtain data required for the characterisation of the municipal wastewater into its fractions. These were entered in the simulation software, BioWin® (EnviroSim, Canada). Historical laboratory and online sensor data, acquired from the utility's data management system, was used for the calibration of the biokinetic model. Initially, the model was calibrated for the effluent quality and then subsequently for N_2O emissions. Finally, the calibrated model parameters and predictions related to effluent quality and N_2O emissions were analysed and interpreted. In the below sub-sections, an explanation on the model used and calibration methodology is provided.

2.2. Biokinetic model to predict N_2O emissions

2.2.1. N_2O emissions model

The simulation software BioWin was used here to conduct the biokinetic modelling of the wastewater treatment processes and the production of N_2O emissions (Elawwad et al., 2019). BioWin makes use of ASDM, which is divided into six main models that cover the main processes in wastewater treatment: activated sludge modelling, anaerobic digestion model, settling models, chemical precipitation modelling, pH modelling, and an aeration and gas transfer model (Elawwad et al., 2019). We used here the built-in N_2O model available in the BioWin ASDM model. N_2O production appears to be driven by elevated levels of

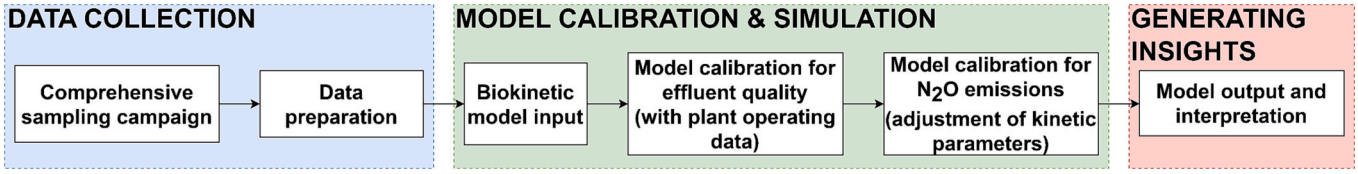

Fig. 2. Overview of the methodology employed in this study.

NO_2^- concentration and therefore, its occurrence as an intermediate product in nitrification and denitrification forms a basis for modelling the N_2O generation (Houweling et al., 2011). Over the years, the N_2O model in BioWin has been updated to include the above-described three pathways of N_2O production (EnviroSim: Personal communication), as compared to the previous version reported in Houweling et al. (2011). The two pathways associated with AOB activity during the nitrification process were individually included. The third pathway, associated to incomplete heterotrophic denitrification, was also updated. In Fig. 3, an outline of the AOB growth processes is described, which lead to N_2O production via these pathways.

The base AOB growth rate expression when not considering N_2O production during the first stage of nitrification has been modelled as,

$$AOB_{BaseRate} = \mu_{max,AOB} \times X_{AOB} \times \frac{S_{NH_4^+}}{S_{NH_4^+} + K_{NH_4^+}} \times \frac{S_{O_2}}{S_{O_2} + K_{O_2,AOB}} \quad (1)$$

where, $\mu_{max,AOB}$ is the maximum growth rate of AOB, X_{AOB} is the concentration of AOB in the biomass, $S_{NH_4^+}$ is the concentration of ammonia nitrogen, $K_{NH_4^+}$ is the half-saturation concentration for NH_4^+ as AOB growth substrate, S_{O_2} is the concentration of dissolved oxygen (DO), and $K_{O_2,AOB}$ is the half-saturation concentration of DO for the growth of AOB. The hydroxylamine pathway is directly modelled based on the concentrations of NH_4^+, that serves as the reductant in the conversion to NH_2OH, and is henceforth stated as the *nitrification by-product* pathway. A logistic switching function is defined for this pathway, which takes the form:

$$SW_{AOB,N_2O} = \frac{1}{\left(1 + e^{\left(SW_{AOB,ByProd} \times \left(S_{NH_4^+} - S_{NH_4^+,MaxByProd}\right)\right)}\right)} \quad (2)$$

where, SW_{AOB,N_2O} is referred to as the fraction of AOB producing N_2O from NH_4^+. $SW_{AOB,ByProd}$ is a kinetic parameter referred to as the *by-product of NH_4^+ logistic slope*, which determines the transition between the production of the N_2O by-product from NH_4^+ and the absence of this by-product. When no N_2O by-product is produced, NH_4^+ is subsequently further oxidised to NO_2^-. The kinetic parameter $S_{NH_4^+,MaxByProd}$, is referred to as the *by-product NH_4^+ inflection point*, or as the NH_4^+ level that will result in half of the maximum NH_4^+ substrate becoming N_2O, as a by-product of nitrification. The approach to this production pathway is an adaptation of the kinetics proposed in Houweling et al. (2011).

During the oxidation of NH_4^+ to NH_2OH and finally NO_2^-, high energy electrons are made available that are used either in the regular aerobic electron transport chain, or alternatively, through a denitrifying electron transport chain (Houweling et al., 2011). The latter is defined as the *nitrifier denitrification* pathway and has been modelled based on the presence of HNO_2 (FNA). FNA is the unionised form of NO_2^- and its concentration is pH dependent. Additionally, FNA is toxic in nature, causing mutagenic effects to cellular DNA (Houweling et al., 2011). Therefore, its accumulation may compel the AOB to reduce FNA. In both cases, FNA then behaves as the terminal electron acceptor (TEA), leading to its reduction to N_2O. For this pathway, a switching function is used,

$$SW_{AOB,Denite} = \frac{S_{HNO_2}}{S_{HNO_2} + K_{HNO_2,Denite}} \times \frac{K_{O_2,Denite}}{K_{O_2,Denite} + S_{O_2}} \quad (3)$$

where, $SW_{AOB,Denite}$ is the fraction of NH_4^+ oxidised by AOB that is denitrified and hence, could lead to the production of N_2O due to HNO_2 being consumed as TEA, instead of N_2O directly being produced from the hydroxylamine pathway. S_{HNO_2} is the concentration of FNA, $K_{HNO_2,Denite}$ is the FNA half-saturation concentration for the AOB biomass denitrification. An inhibition function due to the presence of DO is also included, where $K_{O_2,Denite}$ is the S_{O_2} inhibition parameter below which AOB biomass denitrifies. Such a kinetic approach for AOB denitrification aligns with previous models reported (Guo and Vanrolleghem, 2013; Ni et al., 2011) and is recommended to be included to describe N_2O production by AOB denitrification during low DO concentrations (Ni et al., 2013b).

Following Fig. 3, the total AOB growth rate can be subdivided to AOB aerobic growth at high DO concentrations and AOB denitrification growth at low DO concentrations. Therefore, the fraction of AOB growing via the nitrifier denitrification pathway can be calculated using the $AOB_{BaseRate}$ provided in Eq. (1) and the switching function provided in Eq. (3),

$$AOB_{Denitrification} = AOB_{BaseRate} \times SW_{AOB,Denite} \quad (4)$$

The total AOB growth under aerobic conditions comprises biokinetic processes resulting in the fractions of AOB growth that lead to no N_2O production or to N_2O production from the nitrification by-product pathway. To maintain mass balance, the processes can be described as below,

$$AOB_{Aerobic} = AOB_{BaseRate} \times \left(1 - SW_{AOB,Denite}\right) \quad (5)$$

$$AOB_{Growth,NoN_2OProd} = AOB_{BaseRate} \times \left(1 - SW_{AOB,Denite}\right) \times SW_{AOB,N_2O} \quad (6)$$

$$AOB_{Growth,N_2OProd} = AOB_{BaseRate} \times \left(1 - SW_{AOB,Denite}\right) \times \left(1 - SW_{AOB,N_2O}\right) \quad (7)$$

Using the above equations that describe the fractions of AOB biomass growing via the N_2O production pathways, the mass of N_2O is calculated as per the stoichiometry in BioWin's Gujer Matrix. Finally, the third production pathway of N_2O due to incomplete heterotrophic denitrification was incorporated in the modelling of the denitrification subprocesses. In BioWin ASDM, the denitrification processes have been modelled similar to the four step denitrification models reported previously (Ni et al., 2015; Schulthess and Gujer, 1996). Here, the ordinary heterotrophic organisms (OHOs) are described in a manner that allows for the acceptance of multiple substrates (NO_3^- or NO_2^-) from the bulk concentration in the liquid. The substrates are then processed internally leading to either intermediate outputs or the end-product N_2. With respect to N_2O production during the heterotrophic denitrification processes, the amount of N_2O produced from either substrates NO_3^- or NO_2^- is modelled using a switching function,

$$SW_{OHO,FNA} = \frac{[HNO_2]}{[HNO_2] + Ki_{HNO_2}} \quad (8)$$

where, $SW_{OHO,FNA}$ controls the amount of NO_3^- or NO_2^- that is not completely denitrified to N_2, due to the inhibition caused by the presence of FNA. FNA expressed as $[HNO_2]$ is the molar concentration present in the bulk liquid, and Ki_{HNO_2} is a kinetic parameter that represents FNA inhibition, in mol/L. FNA inhibition of denitrification then leads to

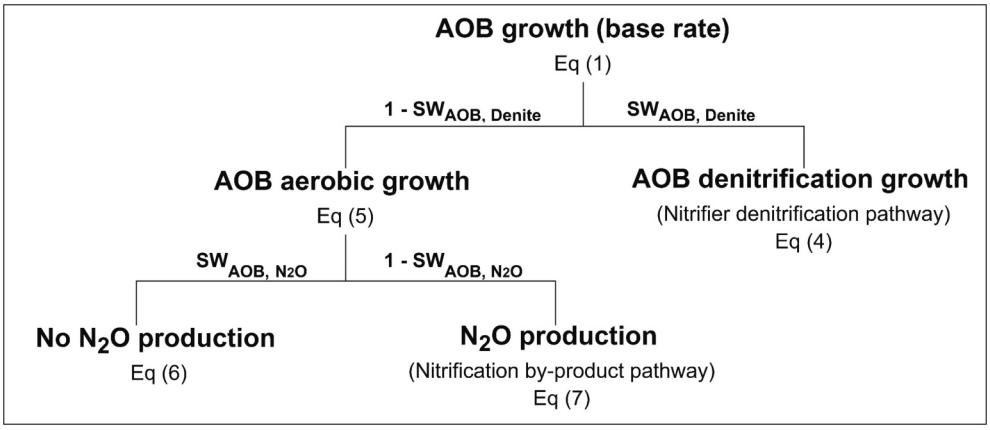

Fig. 3. Flowchart outlining the AOB growth processes while considering the N_2O production pathways associated with AOB where SW represents the various switching functions implemented by BioWin as described in Eq. (2) and (3).

the accumulation of N_2O. Ki_{HNO_2} signifies a threshold concentration, where if the bulk concentration is above this threshold, heterotrophic denitrification is inhibited due to FNA. To provide an example, if Ki_{HNO_2} is reduced, this leads to lower FNA bulk concentrations causing inhibitory conditions. Following Eq. (8), $SW_{OHO,FNA}$ becoming larger and therefore, a larger fraction of NO_3^- or NO_2^- is converted to an end product of N_2O, instead of its reduction to N_2.

2.2.2. Gas–liquid mass transfer of dissolved N_2O concentration

The *Aeration and Gas Transfer Model* implemented in BioWin was used for the interphase transfer of N_2O, from the liquid to the gaseous phase. The mass transfer model is based on the fundamental theory of surface renewal and is formulated as a mass balance. Furthermore, the BioWin mass transfer model adopts certain assumptions in its implementation — (i) the gas and liquid phases are completely mixed with uniform concentrations; and (ii) the gas holdup is considered constant. In applying the mass balance, the saturation concentration and overall mass transfer coefficient of each specie undergoing the gas transfer, including N_2O, is determined. The saturation concentration is calculated using Henry's Law expression which is implemented with a temperature dependency to account for local environmental conditions.

2.3. ASDM-N_2O emissions model calibration methodology

Initially, the process configuration of the treatment process of the full-scale WWTP Amsterdam West (the Netherlands) was mimicked in BioWin by using the physical dimensions of the process units. Using the data from the sampling campaign, a list of the wastewater characteristics specific to the full-scale WWTP's wastewater were mapped into the BioWin ASDM inputs. In addition, long-term laboratory and online sensor data were prepared to be used in the biokinetic model, as detailed in Section 3.2. Data quality control was performed on the datasets. The data was filtered to identify any extreme anomalous/unfeasible values, which were then removed. Gaps in the dataset were filled using a combination of interpolation and by calculating the concentration of the missing days, using the previously available day's mass values and the influent flowrate value available from the online sensor of the specific missing day. For the operating and environmental conditions, available online sensor data for key process parameters were used. The datasets were resampled to daily values for its input into the model. During the calibration procedure, the model fit was evaluated by comparing visually predictions with observed data. More specifically, the assessment involved visual inspection of time series plots of laboratory measurements of effluent quality (Table 5) and online N_2O emissions data. This was conducted to determine the model's capability to accurately capture trends and magnitude of the corresponding variables being predicted.

Necessary adjustments to calibrated kinetic parameter values were made manually to increase the accuracy of predictions. Specifically, the calibration procedure unfolded in two distinct stages:

- *Model Calibration to Predict Effluent Quality*: The model was firstly calibrated to field data representing typical influent wastewater characteristics (such as influent nitrogen load), operating conditions and system performance (such as DO and MLSS concentrations) of the WWTP. Following best practices, steady-state modelling was conducted where physical characteristics of processing units such as the removal efficiency of the primary and secondary settlers, were fine-tuned. This was followed by conducting dynamic simulations where the biokinetic model performance on biological nitrogen removal was assessed. These simulations were conducted using the default BioWin kinetic and stoichiometric parameters. A summary of these parameters can be found in Tables S1–2, in the Supporting Information (SI). Based on the effluent quality predictions assessed in visual plots, specific kinetic parameters were fine-tuned to match the observed effluent quality. Additionally, the sludge retention time (SRT), and hence the wasting of sludge, was controlled. The SRT was calculated by the model, based on the predicted mixed liquor suspended solids (MLSS) concentrations which were very close to the observed values.
- *Model Calibration to Predict N_2O Emissions*: The above model was further calibrated with a goal to achieve accurate predictions of N_2O emissions. Table 1 lists the summary of the N_2O model specific kinetic parameters in BioWin (described in Section 2.2.2) along with their default values that were subject to calibration. As it is not known a priori which N_2O production pathways are active during the seasonal peak, the calibration procedure was conducted on a trial-and-error basis, where the N_2O specific kinetic parameters of each pathway, as provided in Table 1, were individually altered. The kinetic parameters were modified with a goal of triggering the production and emissions of N_2O to match the seasonal peak. The predictions for all four seasons were compared with the available field data using visual plots to assess which N_2O production pathway could provide accurate predictions. The range for alteration of the kinetic parameters was based on expert judgement and values available from limited previous investigations reported in literature. However, careful considerations were given to assess the feasibility of the values that would lead to a reasonable fit with the observed data.

Table 1
N_2O model specific kinetic parameters and their associated N_2O production pathways.

Kinetic parameter	Abbreviation	Unit	BioWin default value	N_2O production pathway
By-product NH_4^+ logistic slope	$SW_{AOB,ByProd}$	–	50	Nitrification by-product
By-product NH_4^+ inflection point	$S_{NH_4^+,MaxByProd}$	mg N/L	1.4	Nitrification by-product
Denitrification DO inhibition parameter	$K_{O_2,Denite}$	mg O_2/L	0.1	Nitrifier denitrification
Denitrification HNO_2 half-saturation	$K_{HNO_2,Denite}$	g N/L	5.00×10^{-6}	Nitrifier denitrification
Free nitrous acid inhibition concentration	Ki_{HNO_2}	mol N/L	1.00×10^{-7}	Heterotrophic denitrification

3. Case study

3.1. Description of WWTP

As mentioned earlier, the case study for this modelling investigation is the Amsterdam West WWTP which has a capacity of 1.1 million population equivalent (168 MLD) (Fig. 4). The raw influent wastewater is initially fed into a grit chamber which is followed by primary settlers. The settled wastewater is distributed to seven treatment lanes to conduct the activated sludge (AS) process for biological nitrogen and phosphorous removal. Due to the availability of the N_2O data in a single lane only, this modelling study was restricted to 1 treatment lane as depicted in Fig. 5. The process configuration applied for the AS is the modified University of Cape Town (mUCT) process. The treatment lane is equipped with a bioreactor, having an anaerobic-anoxic-facultative-aerobic tank in series. The aeration control is executed by establishing the DO setpoint through a table that includes minimum and maximum NH_4^+ concentration setpoints. The DO setpoint rate changes have been defined by the operators of the WWTP. Based on within which NH_4^+ setpoint range the actual NH_4^+ concentrations in the aerobic tank falls within, the DO setpoint is adjusted automatically in (near) real-time. The facultative tank serves the role of a swing tank and is used to increase the denitrification or nitrification potential, based on the treatment requirement. The biologically treated wastewater is then fed into secondary settlers, with decanters being present per treatment lane. Amsterdam West WWTP also possesses an extensive sludge treatment works that was not considered in the modelling and is beyond the scope of this study. However, the flowrate and quality characteristics of the reject water comprised of filtrates from the primary and secondary sludge thickeners and filtrate from the digested sludge thickener after the anaerobic digestor are included in the model (labelled as return streams in Fig. 5). This stream can influence the N_2O emissions due to its relatively high load of N.

3.2. Data

3.2.1. Sampling campaign for wastewater characterisation

The comprehensive sampling campaign in Amsterdam West WWTP was conducted between 11.07.2021–18.07.2021, inclusive. Flow proportional daily composite samples for the raw influent and effluent wastewater were collected using an autosampler. The duration of eight days was deemed sufficient to give multiple data points and provide redundancy of measurements. Furthermore no drastic changes, such as special discharges of wastewater from industries, occurred during the duration of the dataset used for calibration. Therefore, it is expected that the composition and fractions of the wastewater will remain relatively constant (Chen et al., 2023). The following variables were analysed — total chemical oxygen demand (COD), filtered COD, total biological oxygen demand (BOD), filtered BOD, total Kjeldahl nitrogen (TKN), NH_4^+, NO_3^-, total phosphorous (TP), ortho phosphate (Ortho-PO_4^{3-}), total suspended solids (TSS), inorganic suspended solids (ISS) and volatile suspended solids (VSS). All water quality parameter analyses were conducted according to international and Dutch standard methods and protocols, as summarised in Table S3. This data was used to calculate the wastewater fractions relevant to Amsterdam West WWTP's influent wastewater. In Fig. S1, the values entered in the *Influent Specifier* functionality of the BioWin software, are depicted, which provided the characterisation of the domestic wastewater. The resulting list of the wastewater fractions as compared to BioWin's default values can be found in Table S4. Based on the acceptable values obtained, the ASDM model in BioWin was successfully set up to conduct both steady state and dynamic simulations using historical data of the influent and the

Fig. 4. Amsterdam West WWTP (Source: Waternet).

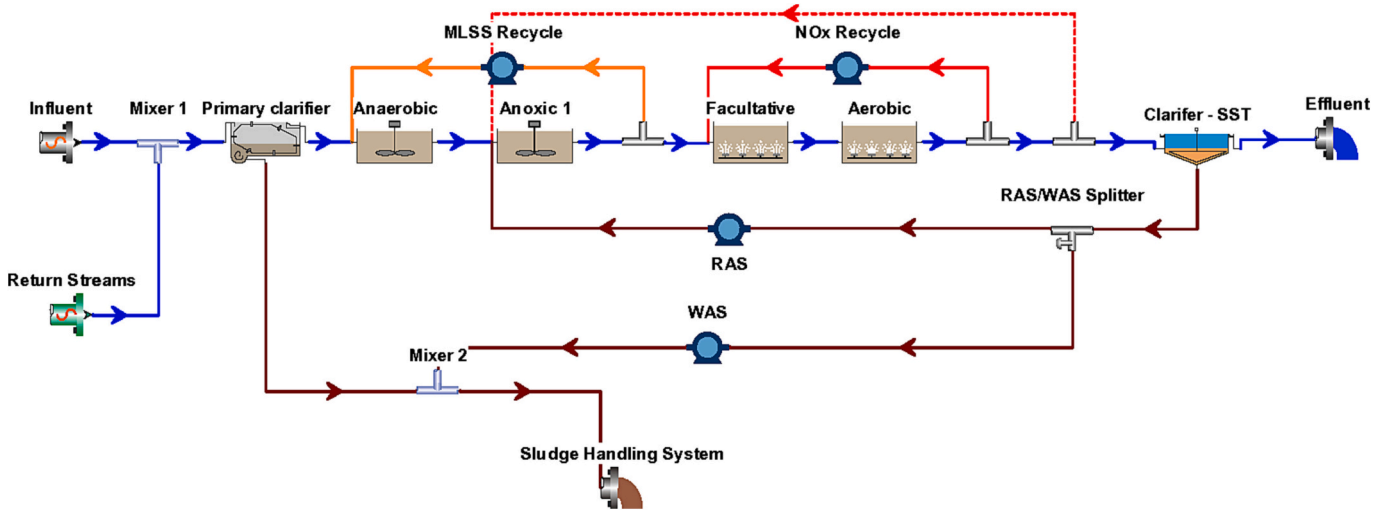

Fig. 5. Amsterdam West WWTP process configuration of 1 treatment lane.

Table 2
Statistics on Amsterdam West WWTP's raw influent wastewater.

Parameter	Unit	Average Yearly Value	Median Yearly Value
Flowrate (1 treatment lane)	m^3/h	989	885
COD	mg COD/L	543	550
BOD	mg BOD/L	247	250
TKN	mg N/L	55	58
TP	mg P/L	7	7
TSS	mg/L	311	300

operational conditions at the Amsterdam West WWTP.

3.2.2. Treatment process data

Historical laboratory measurements and online sensor data amounting to one year for the period 11/2020–10/2021 was used for model calibrations. Laboratory data on the influent and effluent quality, measured on the total volume of water entering and exiting the plant, respectively, and quality data on the sludge reject water streams were used. The following parameters were measured — COD, BOD, TKN, total nitrogen (TN), TP and TSS. The laboratory measurements are based on flow proportional composite samples collected every 3 days by an autosampler. In Table 2 and Table 3, statistics on the raw influent wastewater and treated effluent can be found, respectively. In the investigated treatment lane, installed online sensors, providing high resolution 1 min data on key process parameters was accessed. For the same 1-year period, the influent flowrate, MLSS in the bioreactor, recirculation flowrates, temperature of the mixed liquor, DO concentration in the aerobic tank and facultative tank, return activated sludge (RAS) flowrate, waste activated sludge (WAS) flowrate and the sludge reject water streams flowrate were utilised as input to the biokinetic model. The measured data for the influent COD and TKN, aerobic tank DO and MLSS concentrations, and mixed liquor temperature are provided in Fig. S2.

3.2.3. N_2O emissions data

The bioreactor units of Amsterdam West WWTP are covered, allowing for the capture of the off-gas emissions from the bioreactor and the direct measurements of N_2O concentrations in the gaseous phase from the captured off-gas. Off-gas samples were fed into a non-dispersive infrared gas analyser (X-stream, Emerson, St. Louis, MO, US), which provided measurements every 15 min as a volume fraction (ppmv). These measurements were further processed using off-gases flow measurements to calculate the mass of N_2O emitted from the sampled treatment lane. Further information can be found in Section S.3. By

Table 3
Statistics on the treated effluent quality from Amsterdam West WWTP.

Parameter	Unit	Average yearly value	Median yearly value
COD	mg COD/L	37.0	37.0
BOD	mg BOD/L	2.8	3.0
TKN	mg N/L	3.4	3.0
NH_4^+	mg N/L	1.5	1.0
NO_x	mg N/L	4.2	4.2
TN	mg N/L	7.6	7.3
PO_4^{3-}	mg P/L	0.4	0.2
TP	mg P/L	0.7	0.5
TSS	mg/L	6.3	6.0

exploring the N_2O data for one year, covering all four seasons, a distinctive seasonal peak was found to be occurring during the spring months, as shown in Fig. 6. It was seen that during the months of March and April, 54 % of the yearly emitted mass of 6247 kg of N_2O was emitted from the WWTP. In contrast, low N_2O emissions were seen during the winter and summer seasons. The distinctive peak and the seasonal variations in the N_2O emissions measured in Amsterdam West WWTP were in line with what was observed in other long-term monitoring campaigns (Gruber et al., 2021a).

4. Results

4.1. Model calibration results for effluent quality

Dynamic simulations were performed using the plant operating data while maintaining the default kinetic parameter values, listed in Table S1. The SRT was controlled to 14 days, providing an accurate MLSS prediction in the various bioreactor compartments. However, initial simulations suggested a poor fit for NO_2^- effluent concentration, which was caused by nitrite oxidising bacteria (NOB) biomass, predictively being washed out. Therefore, certain NOB related kinetic parameters were adjusted to better fit the observed data, as shown in Table 4.

Conventionally, the DO half saturation constant of AOB ($K_{O,AOB}$) is considered lower than $K_{O,NOB}$, suggesting that AOB have a higher affinity for oxygen than NOB. In BioWin, the default value for $K_{O,AOB}$ is 0.25 mg O_2/L. However, certain experimental and modelling studies have reported $K_{O,AOB}$ to be higher than $K_{O,NOB}$ (Daebel et al., 2007; Manser et al., 2005; Regmi et al., 2014), corroborating the adjustments necessary during the calibration process of this model. The switch in the DO half saturations between AOB and NOB (i.e., $K_{O,AOB} > K_{O,NOB}$) was

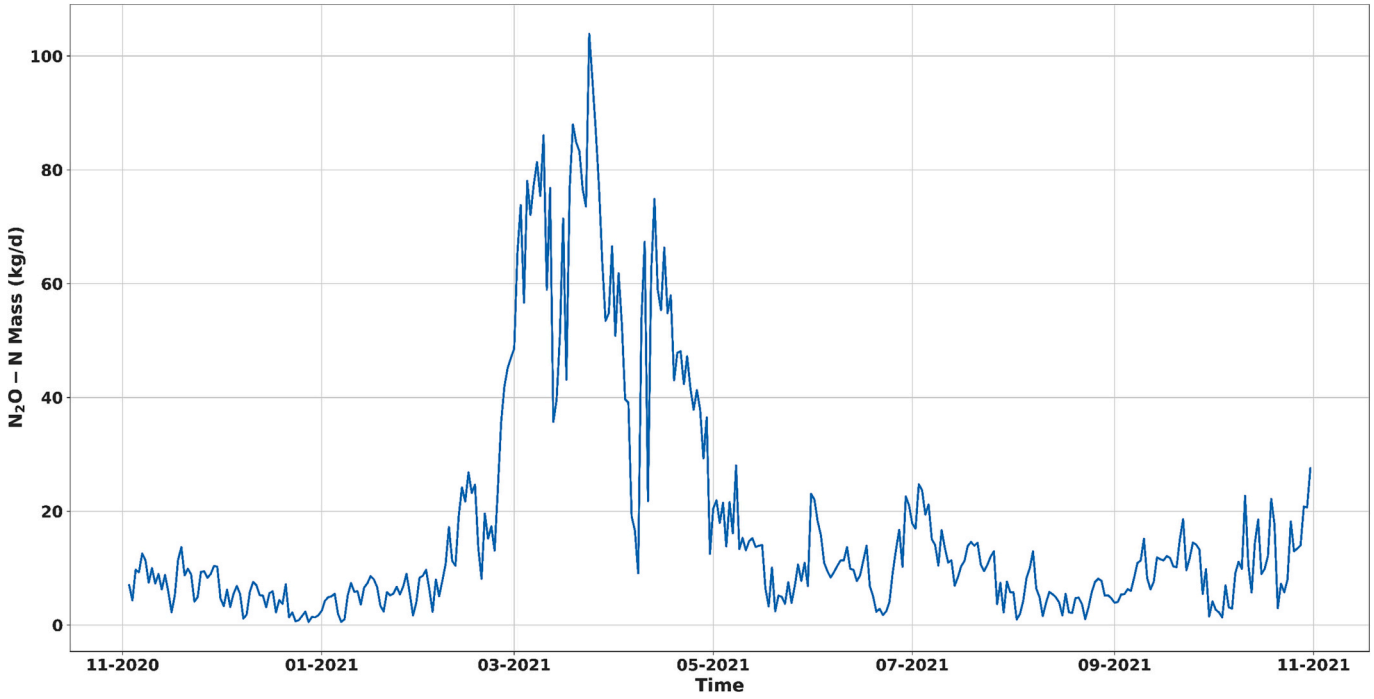

Fig. 6. Seasonal variations of N_2O emissions (kg/d) from 1 treatment lane in Amsterdam West WWTP. A significant seasonal peak between the months 03-2021 and 05-2021 is prevalent.

Table 4
NOB kinetic parameters adjusted to increase fit with observed NO_2^- effluent concentrations.

Kinetic parameter	BioWin default value	Calibrated Value
NO_2^- substrate half-saturation constant (mg N/L)	0.10	0.05
DO half saturation constant – $K_{O,NOB}$ (mg O_2/L)	0.50	0.12
Arrhenius value for maximum specific growth rate	1.06	1.04

particularly found when measurements were made in the floc (Picioreanu et al., 2016). A potential explanation for this switch is due to NOB having a lower oxygen yield and smaller average colony sizes, when compared with AOB (Picioreanu et al., 2016). In Table 5, the yearly averaged results and standard deviations from the dynamic simulations on the effluent quality and MLSS in the aerobic tank are provided and compared with the observed values. The model predictions for COD, TN, TSS and MLSS as compared with observed values can be found in Fig. S3. The dynamic simulations provided satisfactory predictions of the effluent quality values, confirming that the model was successfully calibrated to dynamic conditions. Accordingly, the next stage of calibration to predict the N_2O emissions was started.

Table 5
Effluent quality and aerobic MLSS results from the steady state simulations for Amsterdam West WWTP.

Variable	Yearly averaged observed values (±standard deviation)	Yearly averaged model predictions (±standard deviation)
COD-T (mg/L)	37.0 ± 4.96	30.7 ± 4.61
TN (mg N/L)	7.6 ± 2.40	8.7 ± 2.78
TKN (mg N/L)	3.4 ± 1.50	4.0 ± 1.52
NOx (mg N/L)	4.3 ± 1.78	4.7 ± 2.25
NH_4^+ (mg N/L)	1.5 ± 1.39	2.2 ± 1.46
TSS (mg/L)	6.3 ± 2.59	4.6 ± 0.83
Aerobic tank MLSS (mg/L)	4164 ± 347.98	4388 ± 385.71

4.2. Model calibration results for N_2O emissions

4.2.1. Inactivity of nitrification by-product pathway

Fig. S4, shows the emissions prediction results for several cases. The black line corresponds to the baseline predictions made, using the default N_2O kinetic parameter values listed in Table 1. Results showed that the model is unresponsive to the seasonal peak observed during the spring months leading to the necessity of adjusting the kinetic parameters associated with the N_2O production pathways. Initially, adjustments were made to the kinetic parameters related to the nitrification by-product pathway. The *by-product NH_4^+ logistic slope* ($SW_{AOB,ByProd}$) was changed from its default value of 50 to a range of 25–75. This resulted in minimal effects on the predictions. The second kinetic parameter in this pathway, *by-product NH_4^+ inflection point* ($S_{NH_4^+,MaxByProd}$), was then adjusted. Based on the definition of the parameter within the pathway's kinetic expression, the reduction of this parameter was likely to predict more N_2O. In Fig. S4, the model predictions with adjusting $S_{NH_4^+,MaxByProd}$ to 0.7 mg N/L are shown, depicted as the orange line. Despite a considerable adjustment of this kinetic parameter (from 1.4 to 0.7 mg/L), there was little effect on the prediction accuracy.

4.2.2. Seasonal peak predictions due to multiple production pathways

In the nitrifier denitrification pathway, two kinetic parameters are present in the model to allow for N_2O production; first being the denitrification DO inhibition parameter ($K_{O_2,Denite}$) and second, the denitrification HNO_2 half-saturation constant ($K_{HNO_2,Denite}$). Initially, the $K_{O_2,Denite}$ was increased to ensure that a higher fraction of NH_4^+ oxidised by the AOB was denitrified and therefore, produced more N_2O. In Fig. S4, the green line shows the results obtained by adjusting the parameter to 0.7 mg O_2/L, which is a 7-fold increase compared to the default value of 0.1 mg O_2/L. This adjustment resulted in a moderate fit for the summer and fall seasons, when compared to the simulation

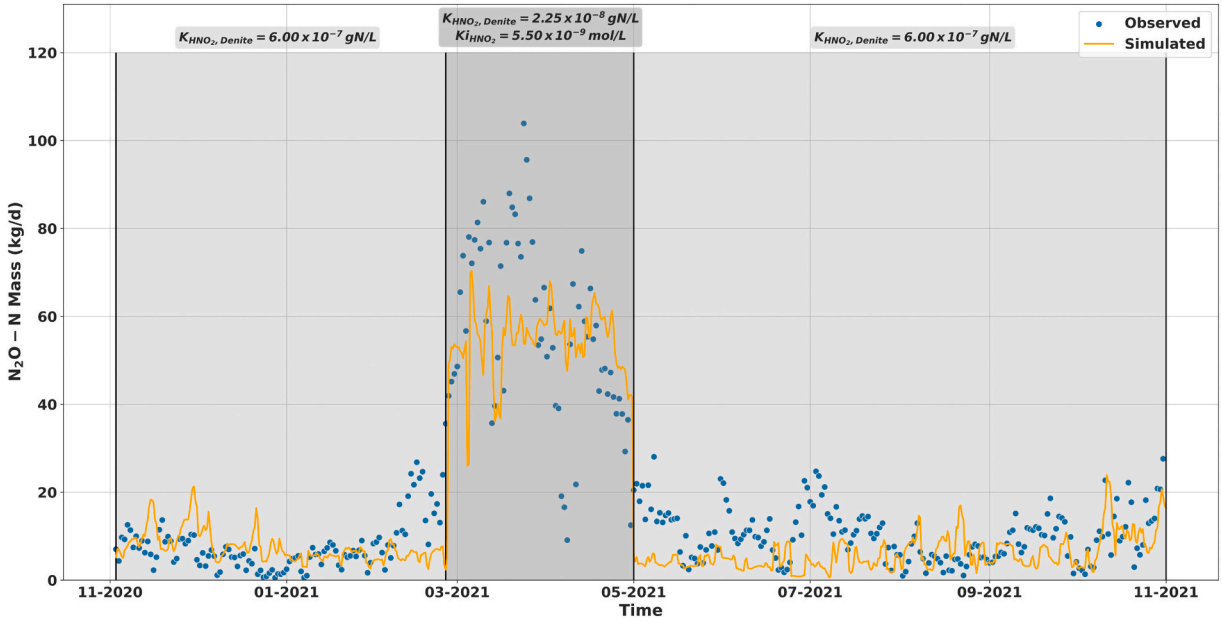

Fig. 7. Predicting the seasonal variations of N_2O emissions with adjustments made to the AOB denitrification HNO_2 half-saturation constant ($K_{HNO_2,Denite}$) and the HNO_2 concentration (Ki_{HNO_2}) leading to the inhibition of the heterotrophic denitrification. The blue dots represent the observed N_2O emissions and the orange line the predictions from the biokinetic model. In the light grey region (winter, summer and fall seasons having low N_2O emissions), the $K_{HNO_2,Denite}$ was adjusted to 6.00 $\times 10^{-7}$ g N/L and in the dark grey region (spring season, presence of seasonal peak), $K_{HNO_2,Denite}$ was modified to 2.25 $\times 10^{-8}$ g N/L and Ki_{HNO_2} to 5.50 $\times 10^{-9}$ mol/L.

Table 6
Summary of N_2O specific kinetic parameters modified in model calibration to predict the seasonal variations of the N_2O emissions from the full-scale Amsterdam West WWTP.

Kinetic parameter	BioWin default value	Modified value	N_2O production pathway
Denitrification HNO_2 half-saturation ($K_{HNO_2,Denite}$)	5.00 $\times 10^{-6}$ g N/L	Seasonal peak: 2.25 $\times 10^{-8}$ g N/L Other seasons: 6.00 $\times 10^{-7}$ g N/L	Nitrifier denitrification
Free nitrous acid inhibition concentration (Ki_{HNO_2})	1.00 $\times 10^{-7}$ mol N/L	Seasonal peak: 5.50 $\times 10^{-9}$ mol N/L	Heterotrophic denitrification

performed with default kinetic parameter values (Fig. S4). However, like the kinetic parameters of the nitrification by-product pathway, the change yielded no response with respect to the observed seasonal peak.

Subsequently, the kinetic parameter $K_{HNO_2,Denite}$, was adjusted, and the model's predictions were assessed for all seasons. The $K_{HNO_2,Denite}$ was reduced from 50.00 $\times 10^{-7}$ g N/L to 6.00 $\times 10^{-7}$ g N/L, based on the ASMG1 model developed by Guo and Vanrolleghem (2013), that includes a modified version of the AOB denitrification model developed by Mampaey et al. (2013). As depicted in Fig. 7, this modification led to a satisfactory fit for the winter, summer and fall seasons. However, the change was insufficient to adequately predict the seasonal peak, observed in spring. Therefore, the $K_{HNO_2,Denite}$ was further decreased to a value of 2.25 $\times 10^{-8}$ g N/L, which is an ~96 % decrease to the parameter value proposed by Guo and Vanrolleghem (2013). This further modification led to an increase in N_2O production although not fully reflecting the observed seasonal peak.

A further decrease of this parameter is non-justifiable based on the uncertainty classification reported in the study conducted by Boiocchi et al. (2017). The authors ranked all kinetic parameters related to the AOB denitrification, including $K_{HNO_2,Denite}$, to CLASS 4 which is defined as 100 % uncertainty, suggesting that the modelling of such processes is still subject to very high uncertainties. This was attributed to the fact that the AOB denitrification kinetic parameters are related to newly identified processes that have been recently introduced to biokinetic models. Therefore, for the prediction of the seasonal peak, the third pathway of incomplete heterotrophic denitrification pathway was considered.

In the model, the production of N_2O emissions due to an incomplete heterotrophic denitrification pathway is influenced by the HNO_2 (FNA) inhibition concentration (Ki_{HNO_2}). This parameter prevents the conversion of NO_3^- and NO_2^- to N_2, hence leading to the accumulation of N_2O. To facilitate the production of more N_2O from the model during the seasonal peak and to achieve a better fit with the observed values, this parameter was adjusted by lowering the inhibition concentration to a value of 5.50 $\times 10^{-9}$ mol/L. In Fig. 7, the prediction of the seasonal peak due to the modification of the $K_{HNO_2,Denite}$ from the nitrifier denitrification pathways as well as the Ki_{HNO_2} is shown in the dark grey region. The combination of these adjustments provided a reasonable prediction for the seasonal peak. However, the modification of the Ki_{HNO_2} to the value of 5.50 $\times 10^{-9}$ mol/L, while providing a better fit for the seasonal peak, lacks scientific justification. Similar to the adjustment of the $K_{HNO_2,Denite}$, the Ki_{HNO_2} was reduced by ~94 %, when compared to the BioWin default FNA inhibition concentration value (Table 6). A further reduction in this parameter is questionable and unjustified without appropriate scientific evidence. This signifies that the current biokinetic model has limitations in accurately predicting the N_2O seasonal peak.

5. Discussion

5.1. Insights on active production pathways during seasonal variations

The calibration of the biokinetic model by modifying certain kinetic parameters indicated which of the proposed N_2O production pathways prevailed in the full-scale WWTP. In Table 6, a summary of the kinetic parameter modifications is given, compared with the default values. During the winter, summer and fall seasons, a modification of the $K_{HNO_2,Denite}$ parameter resulted in a better fit with the observed N_2O emissions. This suggests that in the current biokinetic model approach,

the nitrifier denitrification pathway was prominent during the seasons when low N_2O emissions were observed. Furthermore, the required additional modification of the parameter during the seasonal peak also suggested an increased activation of the nitrifier denitrification pathway during spring, thereby contributing to significant N_2O emissions. The dominance of the nitrifier denitrification pathway corroborates the outcomes reported in earlier investigations (Ni et al., 2013b, 2015). In both cases of low and high N_2O emissions during the various seasons, a reduction in the $K_{HNO_2,Denite}$ parameter was needed. This suggests that a greater fraction of the AOB biomass switches to the denitrifying electron transport chain at lower FNA concentrations than previously perceived. This could be attributed to certain operating conditions such as suboptimal DO concentrations. Alternatively, the AOB might attempt to remove the toxicant FNA itself. Consequently, a greater fraction of the ammonia oxidised by AOB is denitrified at relatively low FNA concentration thresholds, resulting in incomplete nitrification and higher N_2O production.

However, the isolated modifications to the $K_{HNO_2,Denite}$ kinetic parameter of the nitrifier denitrification pathway was insufficient to fit the seasonal peak. Therefore, in the current biokinetic model approach, the additional modification to the FNA inhibition concentration, Ki_{HNO_2}, suggested the prominence of the incomplete heterotrophic denitrification pathway, that causes further production of N_2O. This suggested that the OHOs were required to be more sensitive to FNA and inhibition of the denitrification process is occurring at lower FNA concentrations than previously expected (as set in the default value of the Ki_{HNO_2} kinetic parameter).

The modelling of this WWTP case study highlights the increased presence of FNA as a driving factor in the activation of both prominent pathways, particularly during the seasonal peak. Unfortunately, data on the FNA and NO_2^- concentrations in the mixed liquor of the bioreactor was not available to confirm such a conclusion. However, the availability of NO_2^- data of the total treated effluent from the WWTP, as shown in Fig. 8, provided certain inferences for corroboration. Fig. 8 depicts a clear increase in the NO_2^- concentration in the treated effluent during the N_2O seasonal peak. This suggested an accumulation of the NO_2^- concentration potentially occurring in the bioreactor, which could lead to an accumulation of FNA, based on the pH conditions of the mixed liquor.

It could be hypothesised that during the seasonal peak, AOB denitrification occurs due to increased FNA concentrations and the high sensitivity to FNA. Additionally, the increased FNA concentrations resulted in increased inhibition of the last step of heterotrophic denitrification, which in turn can lead to further increase in N_2O production. While, there is limited understanding as to the causes of the increased NO_2^- or FNA concentrations prior to the seasonal peak, certain hypotheses have been made, such as the disappearance of the NOB population during the peak and its re-establishment, being associated with a population shift (Gruber et al., 2021b). The washout of the NOB population could explain the accumulation of NO_2^-, however for a more solid support of this hypothesis, increased data collection is required on FNA concentrations and microbial population dynamics during a seasonal peak.

5.2. Limitations of ASDM-N_2O biokinetic model

Results from model calibration indicated various limitations in the current biokinetic model. For instance, the model predictions were inaccurate and unresponsive to varying operating and environmental conditions when using the default values of the N_2O model specific kinetic parameters (Fig. S4). Such a result might be attributed to the fact that the default values available in BioWin were calibrated on datasets obtained from bench-scale studies conducted under controlled environments with summer-like conditions, without the occurrence of an identified peak (Houweling et al., 2011; Shiskowski, 2004). However, the increased use of data in our current research was insufficient to acquire accurate predictions of the N_2O emissions covering all seasons.

The role of FNA requires better understanding with respect to its effect on nitrification and denitrification processes and subsequent N_2O production. Furthermore, there is not yet a consensus on what the boundary values of the FNA inhibition concentration (Ki_{HNO_2}) parameter should be, when considering the seasonal variations. Limited investigations on the inhibition of heterotrophic denitrification due to FNA and related N_2O production, have been conducted (Miao et al., 2018; Zhou et al., 2008, 2011). Previous studies have indicated that FNA likely inhibits N_2O reduction more than NO_2^- (Zhou et al. 2008). The results of this modelling study and limited previous research indicated that FNA could be a main triggering factor in N_2O production. This

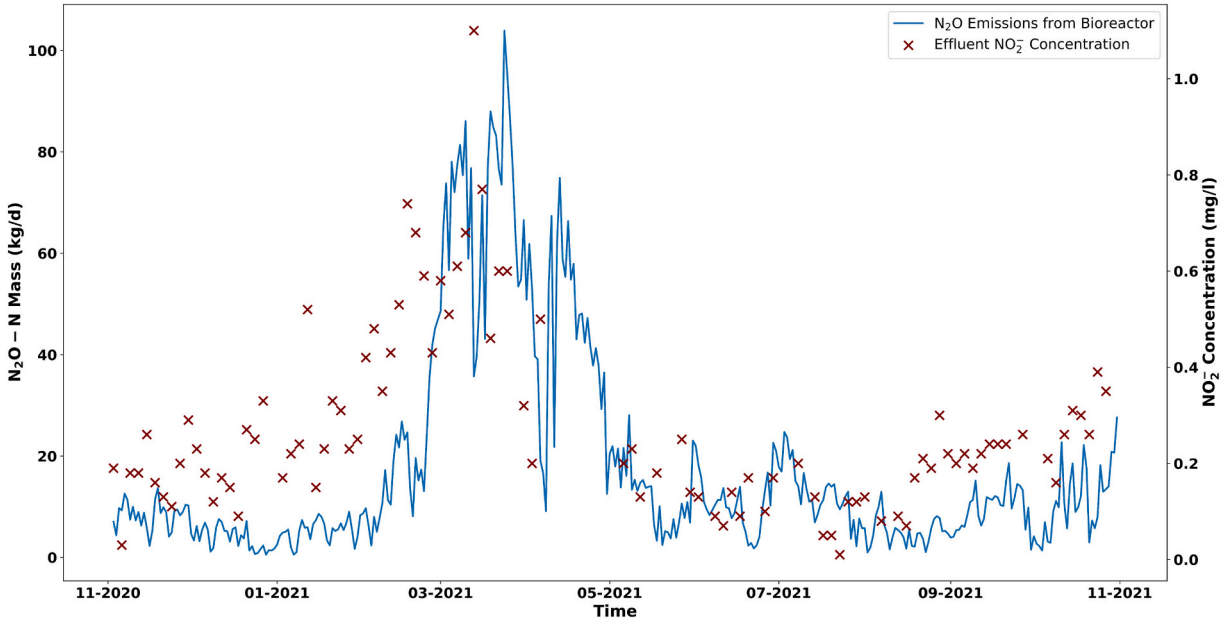

Fig. 8. N_2O emissions from the bioreactor of treatment lane 2 (blue line) and NO_2^- concentration of the overall treated effluent (maroon crosses). During the seasonal peak of N_2O, an increase in effluent NO_2^- concentration is visible.

hypothesis requires in-depth data collection and analysis which in-turn can feed further development and refinement of biokinetic models for N_2O production and emissions.

The current model setup regarding N_2O production kinetics is inflexible to long-term seasonal variations and could be missing key biochemical processes that govern the seasonal variations, such as population dynamics or the presence of other key intermediate compounds as model parameters. Furthermore, the changes to the kinetic parameters specific for the seasonal peak resulted in a bad fit for the other seasons. However, the seasonal peak is a prominent phenomenon in many WWTPs, and therefore the modelling of N_2O emissions must be capable of capturing such dynamics. Furthermore, current biokinetic model implementations group the microorganisms, and do not account for sub-populations of a given bacterial community (such as *Nitrosomonas*, *Nitrospira*, *Nitrosococcus* and *Nitrosolobus*), which could be a limiting factor. Overall, for the biokinetic model to be improved, more understanding on the causes of the N_2O seasonal peak is warranted.

6. Conclusion

In this study, a biokinetic model based on BioWin's ASDM coupled with an N_2O model was setup and calibrated for a treatment lane of a full-scale WWTP in Amsterdam. The model was calibrated using a full year of continuous N_2O emissions data available in the gaseous phase. Based on the results obtained, the key findings are as follows:

- Despite utilising long-term full-scale observed data the current biokinetic model yielded unsatisfactory predictions during the seasonal peak of N_2O emissions. The unsuitability of the default kinetic parameter values provided in the BioWin software became evident during calibration;
- The modelling analysis suggests that for the case of Amsterdam West WWTP, the *nitrification by-product* production pathway did not contribute to predicting the N_2O emissions. This was despite all the changes made to the pathway specific kinetic parameters during the calibration process. Opposite to this, the *nitrifier denitrification* pathway was dominant and active, as evidenced in the acceptable model fit achieved during the winter, summer and autumn (i.e. non-emission peak) seasons;
- It was found that the *nitrifier denitrification* pathway was not unilaterally active during high emissions period, as evidenced in the sub-optimal fit obtained for the spring seasonal peak of N_2O emissions. Incomplete *heterotrophic denitrification* emerged as a significant contributor during this period, as evidenced in a better fit achieved for the seasonal peak when additional modifications were made to the FNA inhibition concentration kinetic parameter (reducing it from 1.00×10^{-7} mol N/L to 5.50×10^{-9} mol N/L); and
- In the current biokinetic model setup the FNA bulk concentration in the mixed liquor influenced the production of N_2O. In this case study, results indicated that the AOB switched to the denitrifying electron chain at lower FNA concentration than initially perceived, to remove the toxic substance, leading to increased N_2O emissions. Similarly, increased FNA concentrations during the seasonal peak, as hypothesised given observed increased effluent NO_2^- concentrations, led to the inhibition of heterotrophic denitrification process causing N_2O production;
- The highlighted limitations of the current biokinetic model are likely stemming from gaps in the understanding and representation of relevant biochemical processes such as the influence of FNA and threshold bulk concentration that leads to the triggering of the N_2O production pathways, and the relation of such processes to temperature and seasonal dependencies.

7. Recommendations

Given the current limitations that biokinetic modelling of N_2O emissions face, we propose that future work should focus on gaining an improved understanding on the causes of the N_2O seasonal peak. Experimental investigations and multi-disciplinary research should be conducted to identify, a feasible range of values for the FNA half-saturation constant and the FNA inhibition concentration, particularly during the N_2O seasonal peak. The identified values of these kinetic parameters will provide an improved understanding on how the increase in FNA concentration results in increased AOB denitrification as well as increased inhibition of the denitrification process. This can be of valuable input to further biokinetic modelling calibration studies that can lead to more accurate predictions of the N_2O emissions.

Furthermore, the current biokinetic models are potentially missing key N_2O production pathways and relevant biokinetic parameters. Moreover, the results of this study suggest that using one year of data was not sufficient to increase the prediction accuracy, even though it was a distinct increase in data duration as compared to previous investigations. As a result, it is recommended that multi-year data for good calibration of biokinetic models should be considered. This is also of importance as the seasonal N_2O emissions peak can shift in time (such as from spring to winter). Alternatively, the use of new technologies such as Artificial Intelligence (AI) modelling could be considered when large amounts of data is available. Preliminary investigations of the use of data-driven modelling have shown promising results for the prediction of N_2O (Hwangbo et al., 2021; Vasilaki et al., 2020). However, while data-driven models could lead to better N_2O emissions predictions, the aforementioned fundamental research will improve our understanding and knowledge of the processes behind the emissions, which is crucial for mitigation strategies.

CRediT authorship contribution statement

Siddharth Seshan: Writing – review & editing, Writing – original draft, Visualization, Software, Methodology, Investigation, Data curation, Conceptualization. **Johann Poinapen:** Writing – review & editing, Validation, Methodology, Conceptualization. **Marcel H. Zandvoort:** Writing – review & editing, Investigation. **Jules B. van Lier:** Writing – review & editing, Supervision. **Zoran Kapelan:** Writing – review & editing, Supervision.

Declaration of competing interest

The authors declare that they have no known competing financial interests or personal relationships that could have appeared to influence the work reported in this paper.

Data availability

Data will be made available on request.

Acknowledgements

We would like to thank the water authority Amstel, Gooi and Vecht, for making their plant WWTP Amsterdam West available for monitoring campaigns. Moreover, we are grateful to them for providing historical laboratory measurement data and online sensor data, including the crucial N_2O emission measurements, which were used for this modelling study. We would like to express our gratitude to Mark Fairlamb of EnviroSim Associates Ltd. for his contribution in the description of the BioWin's N_2O model. This research was funded by the Fiware4Water project, which has received funding from the European Union's Horizon 2020 research and innovation programme under grant agreement No. 821036.

Appendix A. Supplementary data

Supplementary data to this article can be found online at https://doi.

org/10.1016/j.scitotenv.2024.170370.

References

Blomberg, K., Kosse, P., Mikola, A., Kuokkanen, A., Fred, T., Heinonen, M., Mulas, M., Lübken, M., Wichern, M., Vahala, R., 2018. Development of an extended ASM3 model for predicting the nitrous oxide emissions in a full-scale wastewater treatment plant. Environ. Sci. Tech. 52 (10), 5803–5811. https://doi.org/10.1021/acs.est.8b00386.

Boiocchi, R., Gernaey, K.V., Sin, G., 2017. Understanding N_2O formation mechanisms through sensitivity analyses using a plant-wide benchmark simulation model. Chem. Eng. J. 317, 935–951. https://doi.org/10.1016/j.cej.2017.02.091.

Chen, G., van Loosdrecht, M.C.M., Ekama, G.A., Brdjanovic, D., 2023. Biological Wastewater Treatment: Principles, Modelling and Design. IWA Publishing, p. 94. https://doi.org/10.2166/9781789060362.

Chen, X., Tomasz Mielczarek, A., Habicht, K., Holmen Andersen, M., Thornberg, D., Sin, G., 2019. Assessment of full-scale N_2O emission characteristics and testing of control concepts in an activated sludge wastewater treatment plant with alternating aerobic and anoxic phases. Environ. Sci. Technol. https://doi.org/10.1021/acs.est.9b04889.

Daebel, H., Manser, R., Gujer, W., 2007. Exploring temporal variations of oxygen saturation constants of nitrifying bacteria. Water Res. 41 (5), 1094–1102. https://doi.org/10.1016/j.watres.2006.11.011.

Daelman, M.R.J., De Baets, B., van Loosdrecht, M.C.M., Volcke, E.I.P., 2013. Influence of sampling strategies on the estimated nitrous oxide emission from wastewater treatment plants. Water Res. 47 (9), 3120–3130. https://doi.org/10.1016/J.WATRES.2013.03.016.

Daelman, M.R.J., van Voorthuizen, E.M., van Dongen, U.G.J.M., Volcke, E.I.P., van Loosdrecht, M.C.M., 2015. Seasonal and diurnal variability of N_2O emissions from a full-scale municipal wastewater treatment plant. Sci. Total Environ. 536, 1–11. https://doi.org/10.1016/J.SCITOTENV.2015.06.122.

Duan, H., Zhao, Y., Koch, K., Wells, G.F., Zheng, M., Yuan, Z., Ye, L., 2021. Insights into nitrous oxide mitigation strategies in wastewater treatment and challenges for wider implementation. Environ. Sci. Technol. 55 https://doi.org/10.1021/acs.est.1c00840.

Elawwad, A., Matta, M., Abo-Zaid, M., Abdel-Halim, H., 2019. Plant-wide modeling and optimization of a large-scale WWTP using BioWin's ASDM model. J. Water Process Eng. 31, 100819 https://doi.org/10.1016/J.JWPE.2019.100819.

Forster, P., Storelvmo, T., Armour, K., Collins, W., Dufresne, J.-L., Frame, D., Lunt, D.J., Mauritsen, T., Palmer, M.D., Watanabe, M., Wild, M., Zhang, H., 2021. The Earth's Energy Budget, Climate Feedbacks, and Climate Sensitivity. In: Masson-Delmotte, V., Zhai, P., Pirani, A., Connors, S.L., Péan, C., Berger, S., Caud, N., Chen, Y., Goldfarb, L., Gomis, M.I., Huang, M., Leitzell, K., Lonnoy, E., Matthews, J.B.R., Maycock, T.K., Waterfield, T., Yelekçi, O., Yu, R., Zhou, B. (Eds.), Climate Change 2021: The Physical Science Basis. Contribution of Working Group I to the Sixth Assessment Report of the Intergovernmental Panel on Climate Change. Cambridge University Press, pp. 923–1054. https://doi.org/10.1017/9781009157896.00.

Gruber, W., Villez, K., Kipf, M., Wunderlin, P., Siegrist, H., Vogt, L., Joss, A., 2020. N_2O emission in full-scale wastewater treatment: proposing a refined monitoring strategy. Sci. Total Environ. 699, 134157 https://doi.org/10.1016/J.SCITOTENV.2019.134157.

Gruber, W., von Känel, L., Vogt, L., Luck, M., Biolley, L., Feller, K., Moosmann, A., Krähenbühl, N., Kipf, M., Loosli, R., Vogel, M., Morgenroth, E., Braun, D., Joss, A., 2021a. Estimation of countrywide N_2O emissions from wastewater treatment in Switzerland using long-term monitoring data. Water Res. X 13, 100122. https://doi.org/10.1016/J.WROA.2021.100122.

Gruber, W., Niederdorfer, R., Ringwald, J., Morgenroth, E., Bürgmann, H., Joss, A., 2021b. Linking seasonal N_2O emissions and nitrification failures to microbial dynamics in a SBR wastewater treatment plant. Water Res. X 11, 100098. https://doi.org/10.1016/J.WROA.2021.100098.

Guo, L., Vanrolleghem, P.A., 2013. Calibration and validation of an activated sludge model for greenhouse gases no. 1 (ASMG1): prediction of temperature-dependent N_2O emission dynamics. Bioprocess. Biosyst. Eng. https://doi.org/10.1007/s00449-013-0978-3.

Houweling, D., Wunderlin, P., Dold, P., Bye, C., Joss, A., Siegrist, H., 2011. N_2O emissions: modeling the effect of process configuration and diurnal loading patterns. Water Environ. Res. 83 (12), 2131–2139. https://doi.org/10.2175/106143011x13176499923775.

Hwangbo, S., Al, R., Chen, X., Rkan Sin, G., 2021. Integrated model for understanding N_2O emissions from wastewater treatment plants: a deep learning approach. Environ. Sci. Technol. 55 https://doi.org/10.1021/acs.est.0c05231.

Intergovernmental Panel on Climate Change, 2014. In: Team, Core Writing, Pachauri, R. K., Meyer, L.A. (Eds.), Climate Change 2014: Synthesis Report. Contribution of Working Groups I, II and III to the Fifth Assessment Report of the Intergovernmental Panel on Climate Change. IPCC, Geneva, Switzerland, 151 pp.

Kampschreur, M.J., Temmink, H., Kleerebezem, R., Jetten, M.S.M., Van Loosdrecht, M.C. M., 2009. Nitrous oxide emission during wastewater treatment. Water Res. 43, 4093–4103. https://doi.org/10.1016/j.watres.2009.03.001.

Kosonen, H., Heinonen, M., Mikola, A., Haimi, H., Mulas, M., Corona, F., Vahala, R., 2016. Nitrous oxide production at a fully covered wastewater treatment plant: results of a long-term online monitoring campaign. Environ. Sci. Technol. https://doi.org/10.1021/acs.est.5b04466.

Mampaey, K.E., Beuckels, B., Kampschreur, M. J., Kleerebezem, R., Van Loosdrecht, M. C. M., & Volcke, E. I. P. (2013). Modelling nitrous and nitric oxide emissions by autotrophic ammonia-oxidizing bacteria. Environ. Technol., 34(12), 1555–1566. doi:https://doi.org/10.1080/09593330.2012.758666.

Mampaey, Kris E., Spérandio, M., van Loosdrecht, M.C.M., Volcke, E.I.P., 2019. Dynamic simulation of N_2O emissions from a full-scale partial nitritation reactor. Biochem. Eng. J. 152, 107356 https://doi.org/10.1016/j.bej.2019.107356.

Manser, R., Gujer, W., Siegrist, H., 2005. Consequences of mass transfer effects on the kinetics of nitrifiers. Water Res. 39 (19), 4633–4642. https://doi.org/10.1016/j.watres.2005.09.020.

Massara, T.M., Malamis, S., Guisasola, A., Antonio Baeza, J., Noutsopoulos, C., Katsou, E., 2017a. A review on nitrous oxide (N_2O) emissions during biological nutrient removal from municipal wastewater and sludge reject water. Sci. Total Environ. https://doi.org/10.1016/j.scitotenv.2017.03.191.

Massara, T.M., Solís, B., Guisasola, A., Katsou, E., Baeza, J.A., 2017b. Development of an ASM2d-N_2O model to describe nitrous oxide emissions in municipal WWTPs under dynamic conditions. Chem. Eng. J. 335, 185–196. https://doi.org/10.1016/J.CEJ.2017.10.119.

Miao, Z., Li, D., Guo, S., Zhao, Z., Fang, X., Wen, X., Wan, J., Li, A., 2018. Effect of free nitrous acid on nitrous oxide production and denitrifying phosphorus removal by polyphosphorus-accumulating organisms in wastewater treatment. Biomed. Res. Int. https://doi.org/10.1155/2018/9192607.

Ni, B.J., Ye, L., Law, Y., Byers, C., Yuan, Z., 2013a. Mathematical modeling of nitrous oxide (N_2O) emissions from full-scale wastewater treatment plants. Environ. Sci. Tech. 47 (14), 7795–7803. https://doi.org/10.1021/es4005398.

Ni, B.-J., El Ruscalleda, M., Pellicer-N Acher, C., Smets, B.F., 2011. Modeling nitrous oxide production during biological nitrogen removal via nitrification and denitrification: extensions to the general ASM models. Environ. Sci. Technol. 45, 7768–7776. https://doi.org/10.1021/es201489n.

Ni, B.-J., Yuan, Z., Chandran, K., Vanrolleghem, P.A., Murthy, S., 2013b. Evaluating four mathematical models for nitrous oxide production by autotrophic ammonia-oxidizing bacteria. Biotechnol. Bioeng. 110, 153–163. https://doi.org/10.1002/bit.24620/abstract.

Ni, B.-J., Pan, Y., Van Den Akker, B., Ye, L., Yuan, Z., 2015. Full-scale modeling explaining large spatial variations of nitrous oxide fluxes in a step-feed plug-flow wastewater treatment reactor. Environ. Sci. Technol. 49, 42. https://doi.org/10.1021/acs.est.5b02038.

Picioreanu, C., Pérez, J., van Loosdrecht, M.C.M., 2016. Impact of cell cluster size on apparent half-saturation coefficients for oxygen in nitrifying sludge and biofilms. Water Res. 106, 371–382. https://doi.org/10.1016/J.WATRES.2016.10.017.

Ravishankara, A.R., Daniel, J.S., Portmann, R.W., 2009. Nitrous oxide (N_2O): the dominant ozone-depleting substance emitted in the 21st century. Science 326 (5949), 123–125. https://doi.org/10.1126/science.1176985.

Regmi, P., Miller, M.W., Holgate, B., Bunce, R., Park, H., Chandran, K., Wett, B., Murthy, S., Bott, C.B., 2014. Control of aeration, aerobic SRT and COD input for mainstream nitritation/denitritation. Water Res. 57, 162–171. https://doi.org/10.1016/j.watres.2014.03.035.

Schulthess, R.V., Gujer, W., 1996. Release of nitrous oxide (N_2O) from denitrifying activated sludge: verification and application of a mathematical model. Water Res. 30). (3).

Shiskowski, D.M., 2004. Investigation of Nitrous Oxide as a Nitrification Monitoring and Aeration System Control Parameter in Sequencing Batch Reactor Wastewater Treatment Systems. Retrospective Theses and Dissertations, 1919-2007. T, University of British Columbia. https://doi.org/10.14288/1.0063470.

Sin, G., Al, R., 2021. Activated sludge models at the crossroad of artificial intelligence—a perspective on advancing process modeling. Npj Clean Water 4 (1), 1–7. https://doi.org/10.1038/s41545-021-00106-5.

Spérandio, M., Pocquet, M., Guo, L., Ni, B.-J., Vanrolleghem, P.A., Yuan, Z., 2016. Evaluation of different nitrous oxide production models with four continuous long-term wastewater treatment process data series. Bioprocess Biosyst. Eng. 39 https://doi.org/10.1007/s00449-015-1532-2.

Vasilaki, V., Massara, T.M., Stanchev, P., Fatone, F., Katsou, E., 2019. A decade of nitrous oxide (N_2O) monitoring in full-scale wastewater treatment processes: a critical review. Water Res. 161, 392–412. https://doi.org/10.1016/J.WATRES.2019.04.022.

Vasilaki, V., Conca, V., Frison, N., Eusebi, A.L., Fatone, F., Katsou, E., 2020. A knowledge discovery framework to predict the N_2O emissions in the wastewater sector. Water Res. 178, 115799 https://doi.org/10.1016/J.WATRES.2020.115799.

Wunderlin, P., Mohn, J., Joss, A., Emmenegger, L., Siegrist, H., 2012. Mechanisms of N_2O production in biological wastewater treatment under nitrifying and denitrifying conditions. Water Res. 46 (4), 1027–1037. https://doi.org/10.1016/J.WATRES.2011.11.080.

Zhou, Y., Oehmen, A., Lim, M., Vadivelu, V., Ng, W.J., 2011. The role of nitrite and free nitrous acid (FNA) in wastewater treatment plants. Water Res. 45 (15), 4672–4682. https://doi.org/10.1016/J.WATRES.2011.06.025.

Zhou, Yan, Pijuan, Maite, Zeng, Raymond, J., Yuan, Z., 2008. Free nitrous acid inhibition on nitrous oxide reduction by a denitrifying-enhanced biological phosphorus removal sludge. Environ. Sci. Technol. https://doi.org/10.1021/es800650j.